OPEN

Citation: Oncogenesis (2013) **2**, e72; doi:10.1038/oncsis.2013.32

www.nature.com/oncsis

ORIGINAL ARTICLE

Estrogen receptor β activation impairs mitochondrial oxidative metabolism and affects malignant mesothelioma cell growth *in vitro* and *in vivo*

AG Manente[1], D Valenti[2], G Pinton[1], PV Jithesh[3], A Daga[4], L Rossi[5], SG Gray[6], KJ O'Byrne[6], DA Fennell[7], RA Vacca[2], S Nilsson[8,9], L Mutti[10] and L Moro[1]

Estrogen receptor (ER)-β has been shown to possess a tumor suppressive effect, and is a potential target for cancer therapy. Using gene-expression meta-analysis of human malignant pleural mesothelioma, we identified an *ESR2* (ERβ coding gene) signature. High *ESR2* expression was strongly associated with low succinate dehydrogenase B (*SDHB*) (which encodes a mitochondrial respiratory chain complex II subunit) expression. We demonstrate that *SDHB* loss induced *ESR2* expression, and that activated ERβ, by over-expression or by selective agonist stimulation, negatively affected oxidative phosphorylation compromising mitochondrial complex II and IV activity. This resulted in reduced mitochondrial ATP production, increased glycolysis dependence and impaired cell proliferation. The observed *in vitro* effects were phenocopied *in vivo* using a selective ERβ agonist in a mesothelioma mouse model. On the whole, our data highlight an unforeseen interaction between ERβ-mediated tumor suppression and energy metabolism that may be exploited to improve on the therapy for clinical management of malignant mesothelioma.

Oncogenesis (2013) **2,** e72; doi:10.1038/oncsis.2013.32; published online 23 September 2013

Subject Categories: Cancer metabolism

Keywords: estrogen receptor beta; mesothelioma; mitochondria; metabolism; glycolysis inhibitors

INTRODUCTION

Estrogen receptor (ER)-β is the second ER subtype identified in several human tissues traditionally known to be ER negative.[1,2] It has been recently reviewed that ERβ is expressed and exerts anti-proliferative effects in different human tumor models, for example, breast, colon, prostate, T-cell lymphoma, medulloblastoma, glioma and pleural mesothelioma.[3–5] Therefore, drugs with selectivity for ERβ could theoretically suppress tumor growth without having the serious side effects linked to drugs traditionally associated with ERα. To this end, several ERβ-selective agonists have been designed[6–13] that are either in preclinical or early clinical trials.[14,15]

Our group recently demonstrated that ERβ, but not ERα, is expressed in malignant pleural mesothelioma (MMe) cells, where it acts as a tumor suppressor by modulation of the transcription of several genes coding for proteins involved in cell growth control, cell cycle progression and apoptosis, and that its expression is associated with longer patient survival.[16,17]

MMe is a rare but increasingly prevalent, highly aggressive cancer with poor prognosis.[18] The etiology is essentially a function of previous exposure to asbestos fibers, which are considered to be an early-stage carcinogen for MMe that, causing chronic inflammation, may lead to reactive mesothelial hyperplasia and subsequent cancer development.[19,20]

MMe is a highly treatment-resistant and insidious cancer. The current treatment is multimodal, and a patient may receive a combination of chemotherapy, surgery or radiotherapy treatments.[21,22] Patients not eligible for curative surgery receive antimetabolite (Alimta) in combination with cisplatin, which is the standard first-line therapy.[23] This chemotherapeutic combination has, however, moderate efficacy and poor safety profile.[24] There is no defined second-line option. Recent advances in understanding the disease's complex biology have led to moderate improvements in the effectiveness of the standard therapies, resulting in an increase in median survival times.[25,26] However, despite reported improvements in the clinical management of MMe, the unmet need for improved treatment is high. We studied MMe cells as a model to achieve a better understanding of the underlying mechanisms that mediate ERβ anticancer activity and its therapeutic applications focusing on the effects on energy metabolism.

Reprogramming of energy metabolism is one of the hallmarks of cancer. In normal conditions, cells rely on mitochondrial oxidative phosphorylation (OXPHOS) to provide energy for cellular activities. The general enhancement of the glycolytic machinery in various cancer cell lines is well described.[27] The aerobic use of glucose as an energy source through glycolysis in turn leads to a lesser dependence on OXPHOS, which is called the Warburg effect.[28] Although some studies demonstrate a reduction of OXPHOS capacity in cancer cells, other investigations reveal contradictory modifications with the upregulation of OXPHOS

[1]Department Pharmaceutical Sciences, University of Piemonte Orientale 'A. Avogadro', Novara, Italy; [2]CNR-IBBE, Bari, Italy; [3]Liverpool Cancer Research UK Centre, University of Liverpool, Liverpool, UK; [4]IRCCS San Martino-IST, Genova, Italy; [5]Department of Human Morphology and Applied Biology, University of Pisa, Pisa, Italy; [6]Institute of Molecular Medicine, St James's Hospital, Dublin, Ireland; [7]MRC Toxicology Unit, University of Leicester and Leicester University Hospitals, Leicester, UK; [8]Karo Bio AB, Huddinge, Sweden; [9]Department of Biosciences and Nutrition, Karolinska Institutet, Huddinge, Sweden and [10]Department of Medicine, S. Andrea Hospital, Vercelli, Italy. Correspondence: Professor L Moro, Dipartimento di Scienze del Farmaco, Università degli Studi del Piemonte Orientale 'A. Avogadro', via Bovio 6, Novara 28100, Italy.
E-mail: moro@pharm.unipmn.it
Received 5 April 2013; revised 27 June 2013; accepted 16 July 2013

components and a larger dependency of cancer cells on oxidative energy substrates for anabolism and energy production. This apparent conflictual picture is explained by differences in tumor size, hypoxia, and the sequence and repertoir of oncogenes activated.[29–32]

In this study, we aimed to determine the link between ERβ activation and alterations of aerobic energy metabolism. For the first time, we disclose a novel mechanism by which activated ERβ impairs the activity of mitochondrial respiratory chain (MRC) complexes, forcing cells to depend on glycolysis.

Our findings provide an innovative rationale to treat human cancers by selective activation of ERβ, and highlight the potential use of ERβ-selective agonists alone or in combination with glycolysis inhibitors for efficacious malignant mesothelioma therapy with significantly improved side-effect profile.

RESULTS

Expression of *succinate dehydrogenase B* negatively correlates with *ESR2* expression in human MMe cells

In silico analysis of microarray data on biopsies from MMe patients was performed to generate an *ESR2* expression meta-signature. Two publicly available microarray gene-expression data sets from 93 MMe tumors, GSE 2549 ($n=40$) and GSE 29354 ($n=53$) were analyzed. Raw data was pre-processed and normalized using Robust Multichip Average method, and the median expression level for the probe set 210780 was used to stratify the samples into 'High *ESR2*' or 'Low *ESR2*'. Following analysis of variance to adjust for batch variance and find contrast between the two classes, there were 159 probe sets upregulated group and 13 probe sets downregulated in the 'High *ESR2*' group (FDR adjusted $P<0.05$, fold-change $>|2|$). Among downregulated genes, we identified succinate dehydrogenase B (*SDHB),* coding for the B subunit of MRC complex II. The observed negative correlation between *ESR2* and *SDHB* expression was validated by ERβ and SDHB western blot analysis of tissue samples ($n=20$) from MMe patients with different histological subtypes. Densitometric analysis and a representative western blot are shown in Figures 1a and b. To establish whether it is *ESR2* that control *SDHB* expression, we evaluated both SDHB mRNA and protein levels in the MMe-derived REN cells transfected with vectors to over-express or silence *ESR2*. We observed that *ESR2* modulation did not influence *SDHB* gene transcription (Figure 1c), even though there was a negative correlation between ERβ and SDHB-expressed proteins (Figures 1d and e). In order to validate *in vivo* data, we investigated whether *SDHB* silencing in REN cells could affect *ESR2* gene expression. Quantitative real-time PCR (Figure 1f) and western blot analysis (Figures 1g and h) documented a significant increase in both *ESR2* transcription and in ERβ-expressed protein in *SDHB*-silenced cells.

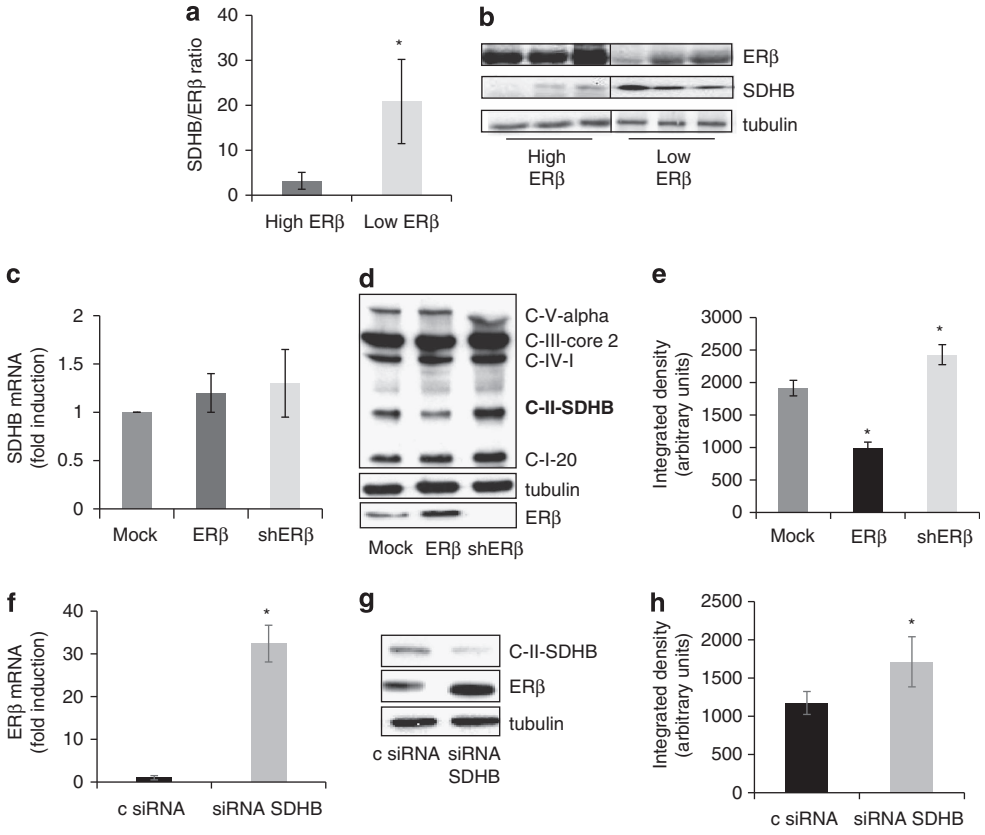

Figure 1. ERβ expression inversely correlates with SDHB expression. (**a**) Bar graph showing the densitometric ratio of SDHB to ERβ evaluated by western blot analysis in tissue samples from MMe patients with different histological subtypes (total number: 20). 'High' or 'low' expressors were defined using the same criteria used for mRNA meta-analysis. (**b**) A representative western blot analysis of ERβ and SDHB expression in tissue samples. (**c**) Relative SDHB mRNA levels measured by real-time PCR in Mock, ERβ over-expressing (ERβ) and ERβ-silenced (shERβ) REN cells. (**d**) A representative western blot analysis of MRC subunits expression in Mock, ERβ over-expressing and ERβ-silenced REN cells. (**e**) SDHB quantitative densitometry of the western blot analysis. (**f**) ERβ mRNA expression evaluated by real-time PCR in non-specific control siRNA (c siRNA) or SDHB-silenced (siRNA SDHB) REN cells. (**g**) Western blot analysis of ERβ and SDHB expression in non-specific c siRNA and SDHB-silenced REN cells. (**h**) ERβ quantitative densitometry of the western blot analysis. Each graph is representative of three independent experiments. Each bar represents mean ± s.d. $^*P<0.05$.

SDHB silencing causes alterations in the activity of MRC complexes without affecting cell proliferation

To study the impact of SDHB subunit loss on mitochondrial function *in vitro*, *SDHB* was silenced by transient small interfering RNA (siRNAs) transfection of REN cells. A dramatic reduction in complex II, a noticeable decrease in complex III and a slight increase in complex IV activities were observed (Figure 2a). This confirms the fundamental role of the SDHB subunit for the activity of complex II and, in part, also for complex III, whereas the increased activity of complex IV can be regarded as a secondary compensatory effect to the inhibition of complex II and III.[33,34]

It has been shown that respiratory chain dysfunctions could lead to an increase in compensative mitochondrial biogenesis.[35–37] In our studies, we could demonstrate that *SDHB* silencing led to a significant increase in the number of mitochondria, as assessed by electron microscopy analysis, and in mitochondrial mass (Figures 2b and c). As demonstrated by real-time PCR (Figure 2d), the observed increases corresponded to a rise in the mitochondrial DNA (mtDNA) content, confirming mitochondrial biogenesis. On the basis of our previous data, documenting the role of ERβ as tumor suppressor in MMe,[16,17] we expected a reduction in the growth rate of *SDHB*-silenced cells beause of the

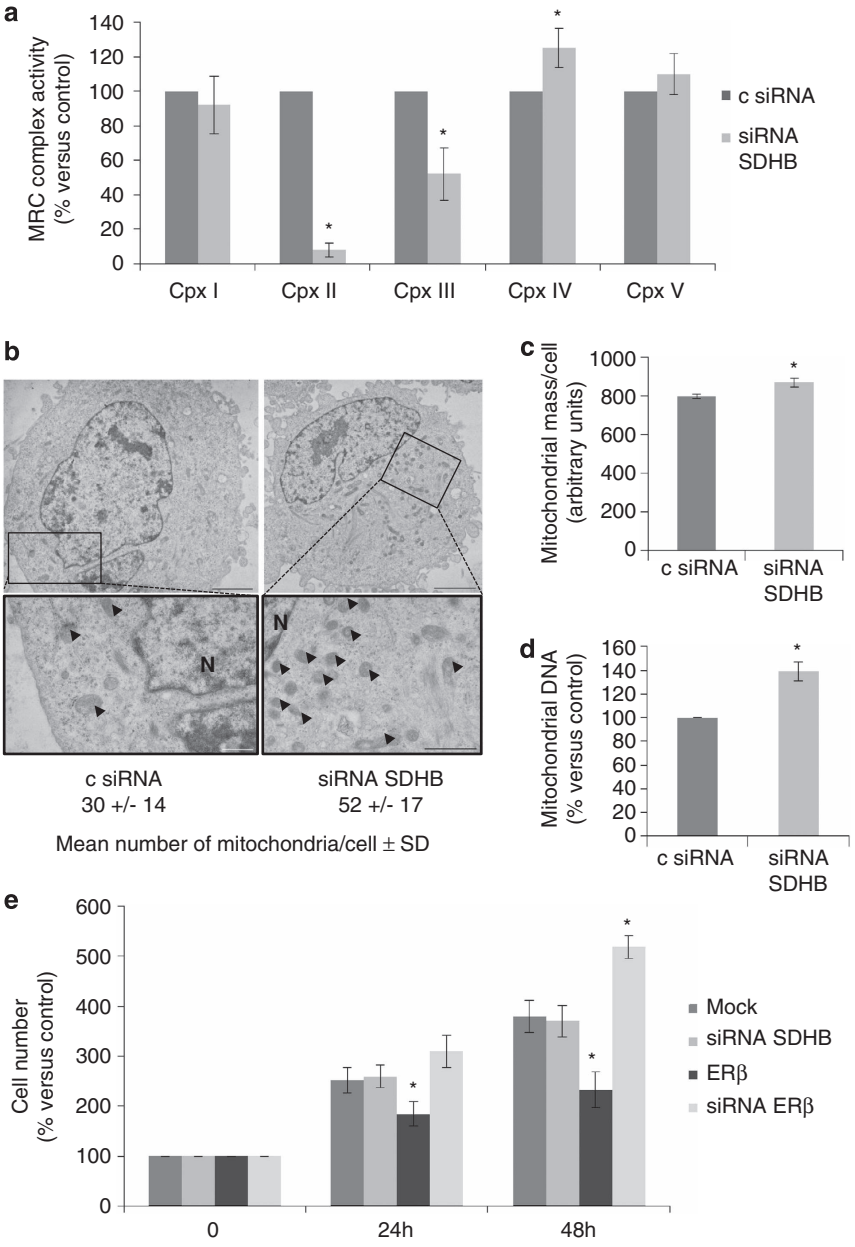

Figure 2. *SDH*B silencing leads to alteration in the activity of MRC complexes, mitochondrial biogenesis but not cell proliferation. (**a**) Spectrophotometric evaluation of MRC complexes enzymatic activities in non-specific control siRNA (c siRNA) and SDHB- (siRNA SDHB) silenced REN cells. (**b**) Electron microscopy analysis performed to observe mitochondrial number and morphology in non-specific control siRNA and SDHB-silenced REN cells. Arrowheads indicate some of the mitochondria, scale bars correspond to 2.5 μm in top left, 3.33 μm in top right, 0.5 μm in bottom left and 0.66 μm in bottom right. N, nucleus. (**c**) Mitochondrial mass per cell determined in c siRNA and SDHB-silenced REN cells using the cardiolipin-selective dye, NAO. (**d**) Changes in mtDNA content relative to the nuclear DNA calculated by real-time PCR of the D-loop and ACTB genes in c siRNA and SDHB-silenced REN cells. (**e**) Growth curves of REN cells transfected with empty vector (Mock), SDHB siRNA, ERβ expression vector (ERβ) or ERβ siRNA at 24 and 48 h. Each bar represents mean ± s.d. *$P < 0.05$.

strong increase in ERβ expression. However, the cell proliferation analysis clearly showed that, differently from ERβ over-expression or silencing, the transient knockdown of *SDHB* did not affect cell growth compared with control cells (Figure 2e).

SDHB silencing in the presence of ERβ activation augments alterations in the activity of MRC complexes and affects cell growth

To get an understanding for the lack of effect on cell proliferation after transient *SDHB* knockdown, we performed a western blot analysis of cell fractions to determine the localization of ERβ in *SDHB*-silenced cells. ERβ, when over-expressed by transient transfection, was predominantly found in the nucleus, while, when induced by *SDHB* silencing, it was mainly retained in the cytosol and translocated to the nucleus only upon activation by its selective ligand KB9520 (Figure 3a). Activation of ERβ by KB9520 and diarylpropionitrile (DPN), two different selective ligands, resulted in strong impairment of complex II and IV activity both in control and *SDHB*-silenced cells (Figure 3b). Real-time PCR analysis demonstrated that ERβ activation by over-expression or binding of selective ligands resulted in the reduced expression of *COX7AR*, which is a nuclear gene coding for an assembly subunit of complex IV, necessary for its full activity (Figure 3c). Over-expression of ERβ mutated in the DNA-binding domain (DBD) opposed the repressive effects of wild-type ERβ on *COX7AR* expression, supporting an important role of ERβ DBD in the transcriptional regulation of *COX7AR* (Supplementary Figures 1A–C). No variations in *COX2*, *COX4.1* and *COX4.2* subunits expression were observed under these conditions (data not shown). Furthermore, ERβ activation by KB9520 impaired proliferation of *SDHB*-silenced cells (Supplementary Figure 2A). Importantly, KB9520 and DPN did not severely impair MRC complex II and IV activities, *COX7AR* expression or cell proliferation of normal ERβ-positive mesothelial MET5A cells (Supplementary Figures 3A–C) and human mesothelial cells (HMC; data not shown), suggesting that selective agonist activation of ERβ is not cytotoxic to normal cells.

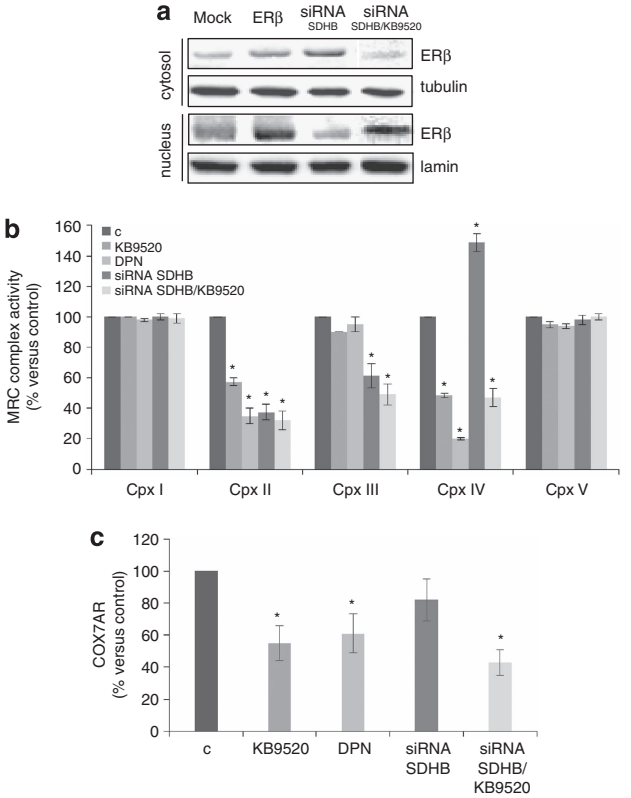

Figure 3. ERβ activation affects MRC complexes activity *in vitro*. (**a**) ERβ western blot analysis of cytosolic and nuclear fractions derived from REN cells, transfected with empty vector (Mock), ERβ expression vector (ERβ) or with SDHB siRNA treated ± 10 nm KB9520, for 1 h. (**b**) Spectrophotometric evaluation of MRC complexes enzymatic activities in wild-type or SDHB-silenced REN cells, treated with 10 nm KB9520 or DPN, for 24 h. (**c**) COX7AR expression evaluated by real-time PCR experiments in wild-type and SDHB siRNA REN cells treated ± 10 nm KB9520 or DPN for 24 h. Each value represents mean ± s.d. $^*P < 0.05$.

ERβ activation compromises the activity of MRC complexes and tumor growth *in vivo*

To reinforce the role of ERβ as a pivotal factor in ERβ-positive tumor cells bio-energetic homeostasis, the *in vitro* studies were repeated in a mesothelioma *in vivo* model. Six-week-old CD1 nude male mice were inoculated with 2×10^6 REN or 1×10^6 MSTO-211H MMe cells by intraperitoneal (i.p.) injection (7 animals/group). Before inoculation, the MMe cells were transduced with a lentiviral vector carrying the luciferase gene to allow imaging in live mice. Fifteen days after cell inoculation, tumor incidence in the peritoneal cavity was 100% in all animal groups. The ERβ-selective agonist KB9520 (10 mg/kg body weight/day), dissolved in the vehicle, was administrated once daily by subcutaneous injection. Untreated animals were subcutaneously dosed with empty vehicle. Animals injected with the ERβ-negative MSTO-211H cells showed a dramatic increase of tumor growth that was not reduced by KB9520 treatment compared with MSTO-211H vehicle control mice (Figures 4a and b). Animals in these treatment arms had to be killed after 10 days of treatment due to their massive tumor growth. In contrast, KB9520 treatment of mice injected with REN cells, which express endogenous ERβ, resulted in a decrease in tumor dimensions as compared with vehicle controls within 10 days of treatment (Figures 4a and b). In 2 out of 7 KB9520-treated mice, a reduction in initial tumor mass was observed after 20 days of treatment, whereas 5 out of 7 mice KB9520 inhibited the rate of tumor growth as compared with vehicle control mice. Treatment with KB9520 was not toxic to the animals as assessed by monitoring changes of mice body weights during the 20 days drug administration. After 35 days from inoculation, all animals were killed. *In vivo* treatment of REN cell tumors with daily doses of KB9520 resulted in upregulation of ERβ at both mRNA and protein levels (Supplementary Figures 4A and B). Interestingly, in tumor tissues recovered from REN-injected mice, 20 days of KB9520 treatment resulted in a strong impairment in MRC complexes II and IV activities (Figure 4c), confirming results obtained in REN cells *in vitro*. Moreover, as evidenced by real-time PCR experiments reported in Figure 4d, and as observed *in vitro*, the expression of *COX7AR* was reduced in tumor tissues from KB9520-treated REN-injected mice compared with vehicle control mice.

Modulation of ERβ levels affects mitochondrial functions

To stress the role of ERβ in metabolic control, MRC activity was evaluated in REN cells over-expressing ERβ. The results, shown in Figure 5a, provide evidence that very high expression of ERβ strongly impaired complex II and IV activities, and that ERβ silencing, on the contrary, led to a significant increase in complex III and IV functionality. To confirm that alterations in MRC complexes activities had consequences on mitochondrial ATP production, we performed a spectrophotometric measurement of the mitochondrial ATP production in ERβ-silenced and over-expressing cells. We observed that ERβ over-expression significantly reduced mitochondrial ATP production at basal levels and in response to stimuli with complexes I and II substrates (Figure 5b). In contrast, silencing of ERβ led to a marked increase

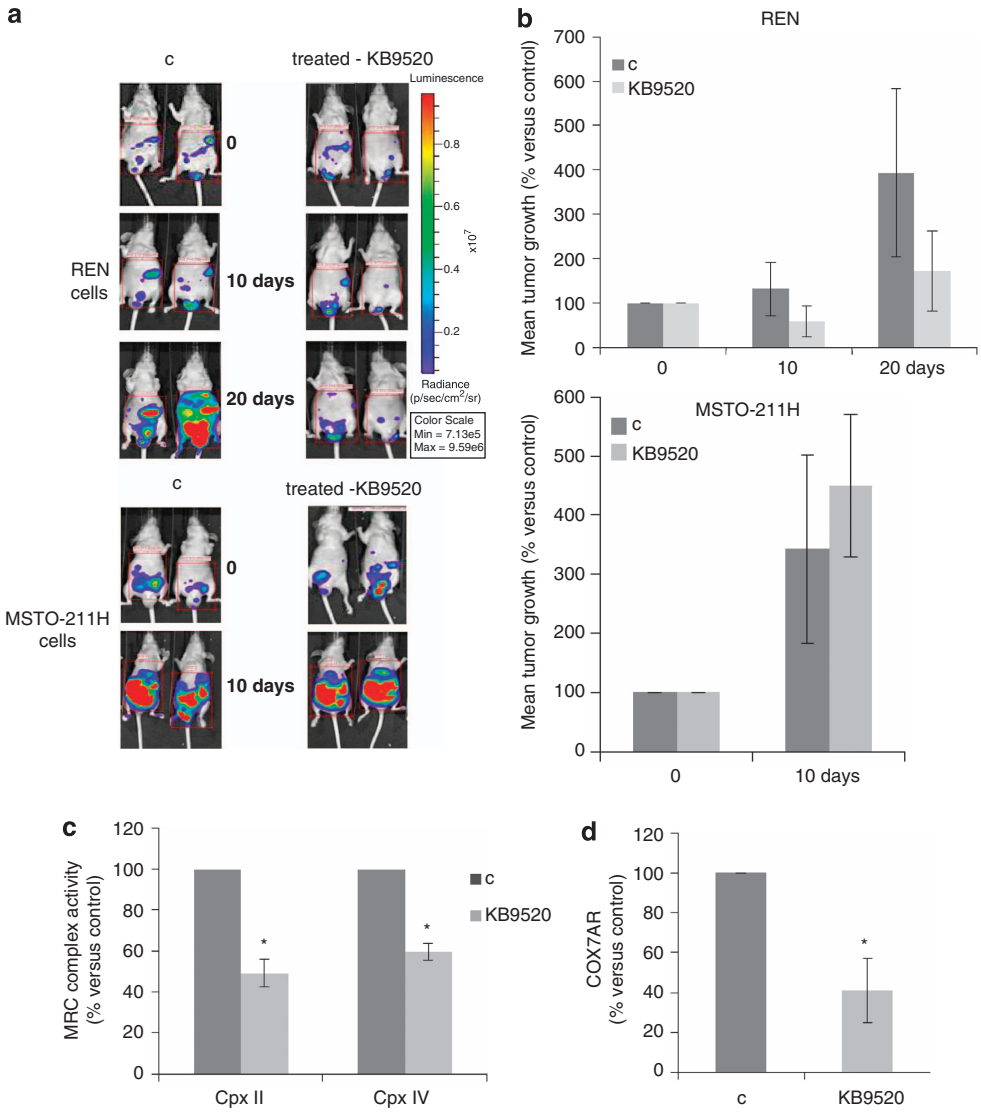

Figure 4. ERβ activation affects MRC complexes activity and tumor growth *in vivo*. (**a**) *In vivo* IVIS imaging to evaluate the progression of peritoneal dissemination of REN/Luc or MSTO-211H/Luc cells implanted in CD1 nude mice, treated with vehicle or KB9520 (10 mg/kg body weight/day) for 10 or 20 days. Representative mice from each treatment group are shown. The color overlay on the image represents the photons per second emitted from the animal in accordance with the pseudo-color scale shown. (**b**) Bar graphs showing the percentages of photon counting increase in control versus treated animals. (**c**) Spectrophotometric evaluation of MRC complex II and IV enzymatic activities in tumors from mice injected with REN cells, treated with vehicle or KB9520 for 20 days. (**d**) COX7AR expression in tumors from mice injected with REN cells and treated with vehicle or KB9520 for 20 days, evaluated by real-time PCR. Each graph is representative of three independent experiments. Each bar represents mean ± s.d. $^*P < 0.05$.

in mitochondrial ATP production both under basal conditions and after stimuli (Figure 5b). In ERβ over-expressing cells, differently from *SDHB*-silenced cells, the alterations in mitochondrial activity were not compensated by an increase in mitochondrial biogenesis, mitochondrial mass or mtDNA content (Figures 5c–e).

ERβ activation sensitizes cells to glycolysis

As ERβ compromises mitochondrial activity, to prove that ERβ over-expressing cells became more glycolysis dependent, we investigated cell growth in glucose-deprived medium. As shown in Figure 6a, ERβ over-expression compromised cell viability in the absence of glucose, supporting the glycolysis dependence of these cells. Moreover, to further explore dependence on glycolysis, we treated ERβ over-expressing, ERβ-silenced and parental REN cells with KB9520 in the presence of the hexokinase inhibitor 2-Deoxy-D-glucose (2DG) or the PFKFB3 kinase inhibitor 3-(3-pyridinyl)-1-(4-pyridinyl)-2-propen-1-one (3PO).[38] In all experimental conditions, glycolysis inhibitors potentiated the effects of over-expressed or KB9520-activated ERβ (Figures 6b and c).

DISCUSSION

Our group has recently demonstrated that the ERβ subtype exerts a key role as a tumor-suppressor gene in MMe.[16,17] In this report, we provide support for an entirely novel mechanism by which activated ERβ interferes with functions of MRC complexes and mitochondrial ATP production in tumor cells (Figure 7).

By *in silico* analysis of microarray data from 93 MMe patients, we generated an *ESR2* expression meta-signature. Among down-regulated genes, as a function of ERβ protein levels, we identified *SDHB* coding for a subunit of the MRC complex II. SDH, also known

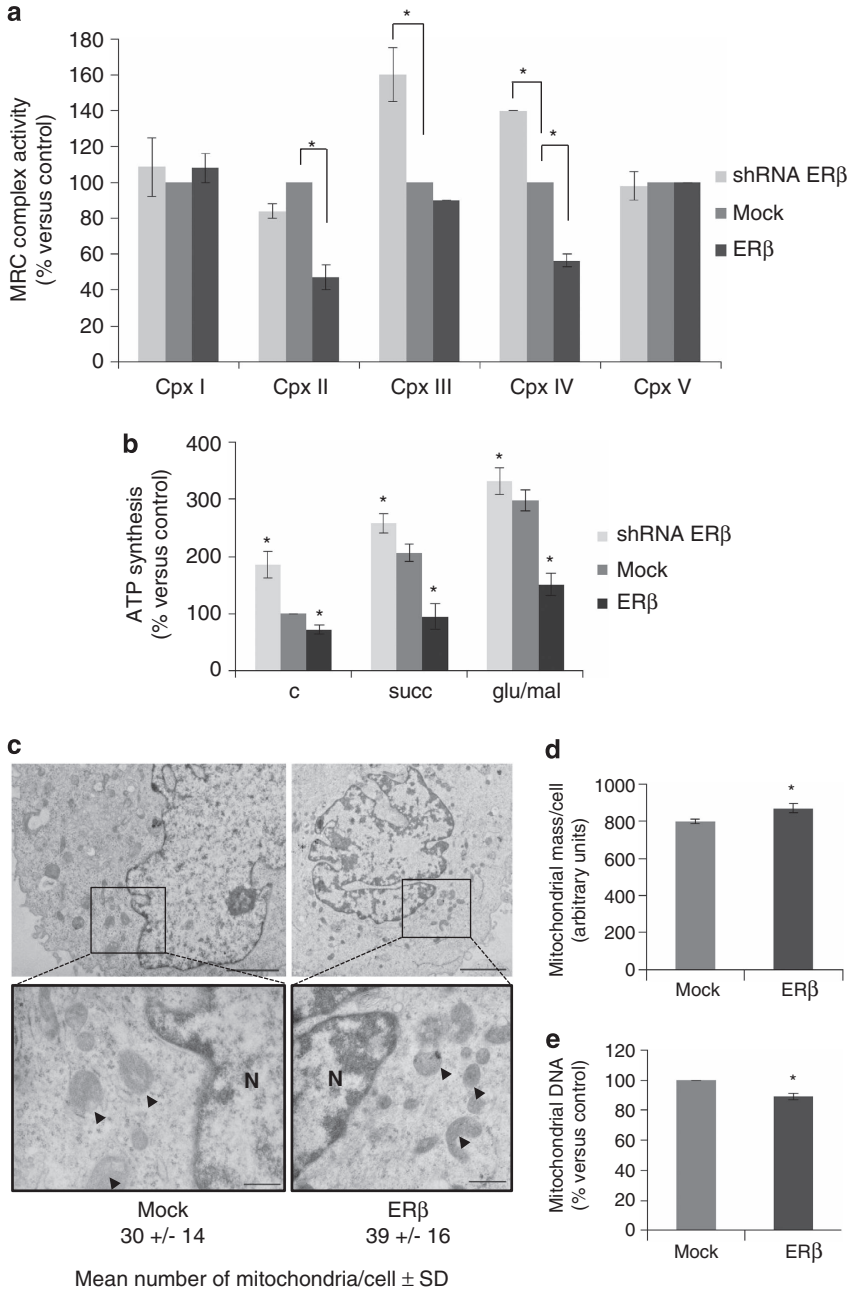

Figure 5. ERβ modulation leads to alterations in mitochondrial functions. (**a**) Spectrophotometric evaluation of MRC complexes enzymatic activities in Mock, ERβ over-expressing (ERβ) or ERβ-silenced (shERβ) REN cells. (**b**) Spectrophotometric determination of mitochondrial ATP synthesis in Mock, ERβ over-expressing or ERβ-silenced REN cells. (**c**) Electron microscopy analysis performed to observe mitochondrial number and morphology in Mock or ERβ over-expressing REN cells. Arrowheads indicate some of the mitochondria, scale bars correspond to 2.5 μm in top left, 3.33 μm in top right, 0.66 μm in bottom left and 1.25 μm in bottom right. N, nucleus. (**d**) Mitochondrial mass per cell measured in Mock and ERβ over-expressing REN cells with the cardiolipin-selective dye, NAO. (**e**) Changes in mtDNA content relative to the nuclear DNA calculated by real-time PCR of the D-loop and ACTB in Mock and ERβ over-expressing REN cells. Each graph is representative of three independent experiments. Each bar represents mean ± s.d. $^*P < 0.05$.

as succinate:quinone oxidoreductase, is a key enzyme in intermediary metabolism and aerobic energy production, coupling the oxidation of succinate in the Krebs cycle to the reduction of ubiquinone in the electron transport chain.[39] The MRC complex II is composed of four nuclear-encoded subunits whose alterations have been related to many different diseases: *SDHA* mutations have been associated to Leigh syndrome, mitochondrial encephalopathy, and optic atrophy[40] and *SDHB*, *SDHC* and *SDHD* alterations have been correlated to hereditary pheochromocytoma and paraganglioma.[41] Also in MMe, the *SDHB* gene locus (1p36.1–p35) has been shown to be significantly altered in copy number.[42] In paraganglioma and pheochromocytoma, sporadic and familial mutations in the *SDHB* gene support a link between mitochondrial dysfunction and tumorigenesis. In contrast, loss of SDHB in the REN malignant mesothelioma cell line is associated with antitumorigenic effects. That knockdown of *SDHB* in REN cells did not result in antiproliferative effects, despite the fact that increased ERβ expression

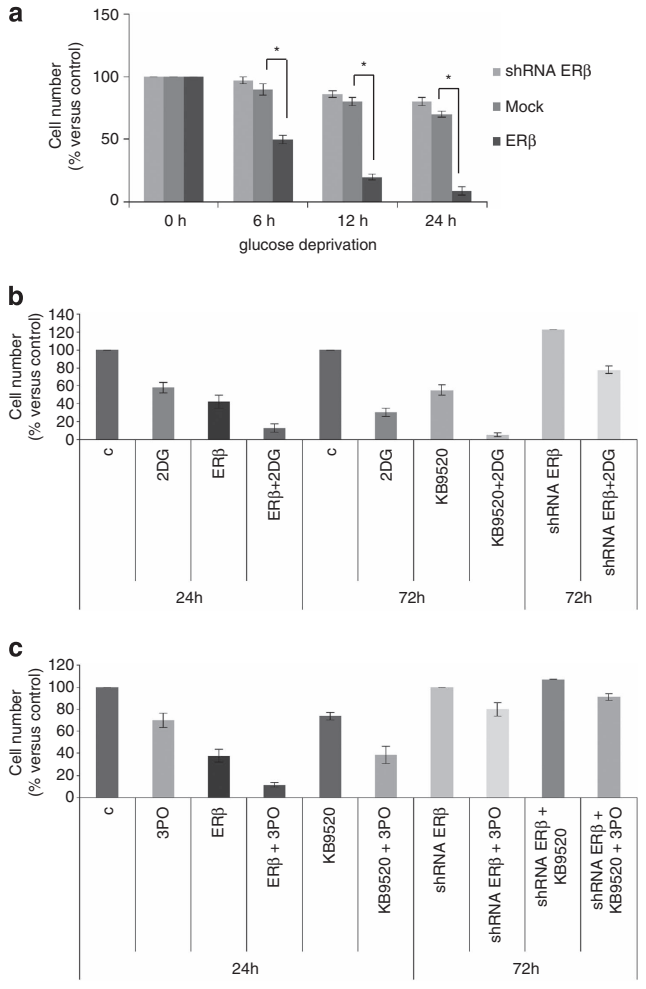

Figure 6. ERβ activation sensitizes cells to glycolysis inhibitors. (**a**) The bar graph compares data of cell survival at different times in a glucose-deprived medium of Mock, ERβ over-expressing (ERβ) or ERβ-silenced (shERβ) REN cells. (**b**) The bar graph compares data of cell count of ERβ over-expressing, wild type in the presence of 10 nM KB9520 (24 h) and ERβ-silenced (72 h) REN cells, treated with 10 mM 2-Deoxy-D-glucose. (**c**) The bar graph compares data of viability of ERβ over-expressing, wild type in the presence of 10 nM KB9520 (24 h) and ERβ-silenced (72 h) REN cells, treated with 10 μM PFKFB3 kinase inhibitor 3PO. Each graph is representative of three independent experiments. Each bar represents mean ± s.d. $^*P < 0.05$.

is best explained by the predominant cytoplasmic localization of ERβ in the absence of ligand activation and the compensatory increase in mitochondrial biogenesis.

The mechanistic explanation for the negative correlation between SDHB and ERβ expression in MMe patients and *in vitro* in the REN MMe cell line is, however, still unknown and needs further exploration.

Cytochrome *c* oxidase is the last and the largest of the MRC complexes, and the assembly of all its 13 subunits is necessary for its full activity; the 11-subunit form, devoid of subunits COX6A and COX6B, retains 85–90% of electron transport activity, whereas the 9-subunit form that lacks two additional subunits (COX3 and COX7AR) has only 40–45% of intact enzyme activity.[43] In this report, we demonstrate that ERβ activation, by over-expression or selective agonist activation, caused a dramatic loss of the MRC complex IV function. The most likely explanation for this effect *in vitro* and *in vivo* is that over-expressed ERβ or activation of ERβ with selective agonists impaired *COX7AR* expression. Mechanistically, this effect of ERβ on *COX7AR* expression is probably mediated by ERβ binding to the perfect palindromic estrogen-responsive element (ERE) identified in the first intron of the *COX7AR* gene.[44] That normal ERβ-positive mesothelial cells did not respond to treatment with ERβ-selective agonists, can be explained by their lower proliferative activity, different energetic profile and/or the presence of co-regulators and other transcription factors that act in concert with ERβ to maintain normal cellular functions.

The observed *in vitro* effects on tumor cells were recapitulated *in vivo* in a MMe mouse model. In contrast to the aggressive tumor growth in mice xenografted with the ERβ-negative MSTO-211H cells and the lack of effect by treatment with KB9520, animals injected with the ERβ-expressing REN cells showed decreased tumor growth rate and tumor volume in response to KB9520. These data further strengthen the role of ERβ as a tumor suppressor, and that the antitumor effect of KB9520 is target specific. Moreover, we could confirm that the KB9520-induced inhibitory effects on MRC complex II and IV, and the repressive effects on *COX7AR* gene expression *in vitro* translates to the *in vivo* mesothelioma tumor model treated with the ERβ-selective agonist KB9520. Interestingly, in tumor tissues recovered from REN-injected mice, treatment with KB9520 resulted in increased ERβ expression at both the levels of transcription and protein, compared with vehicle-treated controls. The mechanism for the increased *ESR2* gene activity is not clear and needs further characterization.

As often observed in numerous forms of cancer, mitochondrial dysfunction may contribute to the preference for glycolysis and glutaminolysis to produce adequate amounts of ATP for cell growth and/or survival.[28,45,46]

We observed that cells in which ERβ was activated, did not present a classical Warburg effect, although they were strongly dependent on glycolysis to survive. These alterations in energy production reflect also their reduced cell proliferation, and this may represent yet another mechanism by which ERβ acts as a tumor suppressor. In fact, the glycolytic pathway produces only two molecules of ATP per molecule of glucose, which is well below the 36 molecules of ATP per molecule of glucose produced by OXPHOS. Consistent with the inhibition of OXPHOS, KB9520 in combination with the hexokinase inhibitor 2-Deoxy-D-glucose or the PFKFB3 kinase inhibitor 3PO, two drugs that target important rate-limiting enzymes in the glycolysis pathway resulted in synergistic inhibition of MMe cell growth.

In summary, our data suggest that treatment with an ERβ agonist alone or in combination with glycolysis inhibitors may be a future strategy for clinical management of ERβ-positive MMe and peritoneal mesothelioma.

MATERIALS AND METHODS

Reagents and antibodies

The monoclonal antibodies specific for α-tubulin, lamin and the polyclonal antibody specific for ERβ were obtained from Santa Cruz Biotechnology (Santa Cruz, CA, USA). The monoclonal antibody for one subunit of each MRC complex (MIX OXPHOS) was obtained from MitoSciences (Eugene, OR, USA). Anti-mouse and anti-rabbit immunoglobulin G peroxidase-conjugated antibodies, 2DG and chemical reagents were obtained from Sigma-Aldrich (St Louis, MO, USA). ECL was obtained from Amersham Pharmacia Biotech (Uppsala, Sweden). Nitrocellulose membranes and protein assay kit were obtained from Bio-Rad (Hercules, CA, USA). Culture media, sera, antibiotics and LipofectaMINE transfection reagent were obtained from Invitrogen (Carlsbad, CA, USA). ERβ-specific agonist DPN was obtained from Tocris (Bristol, UK), and KB9520 and 3PO were provided by Karo Bio AB (Huddinge, Sweden). (KB9520 has been described previously.[14,15] The compound can be obtained following contact with Karo Bio AB and after signing of a Material Transfer Agreement together with a detailed protocol of planned study. A fee covering the cost of compound synthesis will be charged).

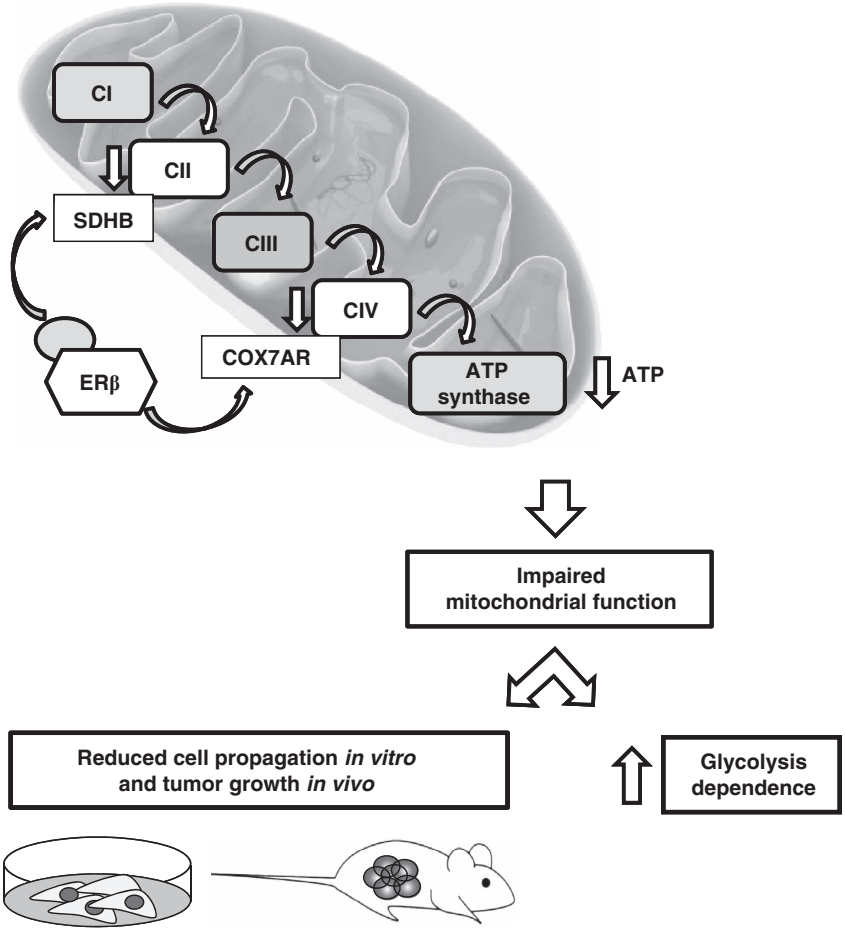

Figure 7. Schematic representation of the proposed mechanism.

Cell cultures and transfection

The epithelioid MMe-derived REN cell line, used as the principal experimental model in this investigation, was isolated, characterized[47] and kindly provided by Dr Albelda SM (University of Pennsylvania, Philadelphia, PA, USA). The biphasic-derived MSTO-211H and the mesothelial MET5A cell lines were obtained from the Istituto Scientifico Tumori (IST) Cell-bank, Genoa, Italy. Cells were cultured in standard conditions. Cells were transiently transfected with the pCNX2 plasmid expressing human wild-type ERβ (Addgene, Cambridge, MA, USA) using LipofectAMINE (Invitrogen) reagent as described by the manufacturer. Gene silencing was achieved using an ERβ-specific shRNA lentiviral plasmid (pLKO.1-puro) (Sigma-Aldrich) or ESR2 and SDHB-specific siRNAs by Qiagen (Hilden, Germany). The plasmid expressing human ERβ mutated in the DBD was kindly provided by Dr Ström A (University of Houston, Houston, TX, USA).[48]

Proliferation assay by cell count

Cells seeded at a density of 10×10^4 cells/well on six-well plates were alternatively treated with the indicated molecules or transiently transfected by the LipofectAMINE reagent, as described by the manufacturer. Cells were then trypsinized and stained with Trypan blue. The number of cells considered viable was counted in a Bürker hemocytometer within 5 min after staining.

Cell lysis and immunoblot

Cells were extracted with 1% NP-40 lysis buffer (1% NP-40, 150 mM NaCl, 50 mM Tris-HCl (pH 8), 5 mM EDTA, 10 mM NaF, 10 mM $Na_4P_2O_7$, 0.4 mM Na_3VO_4, 10 μg/ml leupeptin, 4 μg/ml pepstatin and 0.1 U/ml aprotinin). Cell lysates were centrifuged at 13 000 *g* for 10 min, and the supernatants were collected and assayed for protein concentration with the Bio-Rad protein assay method. Proteins were separated by SDS-PAGE under reducing conditions, transferred to nitrocellulose, reacted with specific antibodies and detected with peroxidase-conjugate secondary antibodies and chemioluminescent ECL reagent. Densitometric analysis was performed using the GS 250 Molecular Image (Bio-Rad).

Preparation of nuclear and cytoplasmic protein fractions

Phosphate-buffered saline-washed cell pellets were resuspended in 10 volumes of buffer 1 (15 mM Tris pH 7.5, 0.8 mM KCl, 0.25 mM EDTA and Sigma protease cocktail). Cells were then allowed to recover for 5 min at 4 °C, and 10% NP-40 was added dropwise. The lysed cells were centrifuged at 1000 *g*. The supernatant (cytoplasmic fraction) was decanted, and the pellet (corresponding to the nuclei) was resuspended in extraction buffer (20 mM Tris-HCl (pH 8.5) 10% glycerol, 2 mM DTT and 0.8 KCl). The DNA was shared by passage through a 25-gauge syringe, and incubated for 45 min on ice. The mixture was centrifuged at 13 000 *g*, and the nuclear fraction was resuspended in 150 mM KCl in extraction buffer. Cellular fractions were analyzed by immunoblotting.

RNA, DNA isolation and quantitative real-time PCR

Total RNA was extracted using the guanidinium thyocianate method.[49] Starting from equal amounts of RNA, cDNA used as template for amplification in the real-time PCR (5 μg), was synthesized by the reverse transcription reaction using RevertAid Minus First Strand cDNA Synthesis Kit from Fermentas–Thermo Scientific (Burlington, ON, Canada), using random hexamers as primers, according to the manufacturer's instructions. As a PCR internal control, *ACTB* was simultaneously amplified using the primers: Fw 5′-CTTCCTTCCTGGGCA-3′ and Rev 5′-TGTGTTGGCGTACAG-3′. The primers sequences for *ESR2* were: Fw 5′-GTCAGGCATGCGAGT-3′ and Rev 5′-GGGAGCCCTCTTTGC-3′; *SDHB* and *COX7AR* primers were

QT00066507 and QT01012368 from Qiagen (Hilden, Germany). For a quantitative analysis of mtDNA content, total genomic DNA was extracted from previously transfected cells using the NucleoSpin kit (Macherey-Nagel, Düren, Germany); primers for *D-loop*, mtDNA sequence and *ACTB* nuclear DNA sequences, obtained from Eurofins MWG Operon (Ebersberg, Germany), were used as described.[50] The real-time reverse transcription–PCR (RT–PCR) was performed using the double-stranded DNA-binding dye SYBR Green PCR Master Mix (Fermentas–Thermo Scientific) on an ABI GeneAmp 7000 Sequence Detection System machine, as described by the manufacturer. Graphical Cycle threshold (*Ct*) values were obtained automatically by the instrument, for each gene tested. Triplicate reactions were performed for each marker and the melting curves were constructed using Dissociation Curves Software (Applied Biosystems, Foster City, CA, USA), to ensure that only a single product was amplified.

Measurement of respiratory chain complexes activities

Measurements of respiratory chain complexes activities were carried out in mitochondrial membrane-enriched fractions from cultured cells or tumor samples. Aliquots of trypsinized cells were washed with ice-cold phosphate-buffered saline, frozen in liquid nitrogen and kept at $-80\,^{\circ}C$ until use. Tumor samples were homogenized in a medium containing 0.25 M sucrose, 2 mM EDTA and 20 mM Tris-HCl, pH 7.5 (20 μl/mg tissue) and centrifuged at 5500 *g*, 3 min at 4 °C. The supernatant was centrifuged twice at 8500 *g*, 10 min at 2–4 °C. Pellet were frozen in liquid nitrogen and kept at $-80\,^{\circ}C$ until use. Isolation of mitochondrial membrane-enriched fractions and measurement of respiratory chain complexes activities were performed essentially as described in ref. 51.

Measurement of mitochondrial ATP production

Cells previously transfected were trypsinized, washed with PBS and suspended in ice-cold sucrose medium (0.25 M sucrose, 10 mM Tris/HCl pH 7.2, 1 mM EGTA and 0.01% (w/v) digitonin), to permeabilize cell membranes as previously described.[52] To measure the mitochondrial ATP production, permeabilized cells (1 mg of protein) were incubated at 37 °C in 1.5 ml of the respiration medium (210 mM mannitol, 70 mM sucrose, 20 mM TRIS-HCl, 5 mM KH_2PO_4/K_2HPO_4 (pH 7.4), 3 mM $MgCl_2$ and 5 mg/ml BSA), with either GLU (glutamate, 5 mM) plus MAL (malate, 5 mM) (complex I substrates) or SUCC (succinate, 5 mM) (complex II substrate). During the analysis, Ap5A (adenylate kinase inhibitor) was added to be sure to measure only the OXPHOS produced ATP.

Preparation of samples for electron microscopy

Cells transiently transfected with the pCNX2 ERβ plasmid, empty vector, *SDHB* siRNAs or non-silencing siRNA were trypsinized, washed with PBS and then fixed in a cacodylate buffer (2.5% glutaraldehyde, 0.1 M cacodylate; pH 7.2) for 2 h at 4 °C. After two washings in cacodylate buffer, 0.1 M samples were processed as described in ref. 53. Ultrathin sections were placed on Formvar carbon-coated copper grids, stained with uranyl acetate and lead citrate, and observed under a Jeol 100 SX transmission electron microscope (Jeol, Ltd, Tokyo, Japan).

Determination of mitochondrial mass

Mitochondrial mass was determined by using the fluorescent dye NAO (10-*n*-nonyl-Acridine Orange; Molecular Probes, Eugene, OR, USA).[54] Sub-confluent cells were trypsinized and resuspended in 0.5 ml of culture medium (5×10^5 cell/ml) supplemented with 25 mM Hepes, pH 7.5, and containing 5 μM NAO. After incubation for 10 min at 37 °C, cells were spun down, washed with ice-cold medium and transferred immediately into a tube on ice for analysis of the fluorescence intensity by flow cytometry. In each measurement, a minimum of 20 000 cells was analyzed. Data were acquired and analyzed on the FL2 channel using CellQuest software (Becton Dickinson, San Jose, CA, USA).

Survival assay in glucose-deprived medium

REN cells seeded at a density of 10×10^4 cells/well on six-well plates and incubated overnight were transiently transfected with the pCNX2 ERβ plasmid, ERβ shRNA and empty vector or siRNA by the LipofectAMINE reagent, as described by the manufacturer. Twenty-four hours later, the transfected cells were grown in a glucose-deprived medium containing galactose. Cells were then trypsinized and stained with Trypan blue. The number of cells considered viable was counted in a Bürker hemocytometer within 5 min after staining.

In vivo experiments

Animals. CD1 nude mice (males, 6 weeks old; Charles River, Calco, Italy) received i.p. injections of 2×10^6 REN or 1×10^6 MSTO-211H luciferase-transduced MMe cells. After anesthetization and i.p. injections of 0.3 ml of 15 mg/ml D-luciferin, tumor dimension and localization of luminescent cells was monitored using the *In Vivo* Imaging System (IVIS) system 100 series (Xenogen Corporation, Hopkinton, MA, USA). Regions of interest were quantified as total photon counts using Living Image software (Xenogen Corporation). To evaluate treatment toxicity, mice were weighed at the start and end of treatments. Mice were killed and necropsied after 20 days of treatment. *In vivo* experiments were approved by Istituto Scientifico Tumori (Genoa, Italy) ethical committee and conform to the relevant regulatory standards.

Drug administration. An elapse of 15 days was allowed for the formation of detectable tumor nodules by IVIS imaging. Mice were then weighed and stratified into each treatment group of seven animals. Treatment protocols were done from the 15th day to the 35th day, and mice were analyzed weekly by IVIS imaging to assess tumor growth. One dose of KB9520 was used (10 mg/kg body weight/day). KB9520 dissolved in the vehicle (5% DMSO/40% PEG 400/55% water) was administrated once daily by subcutaneous administration. Untreated animals were subcutaneously dosed with empty vehicle. At day 35, mice from the two groups were euthanized and necropsied. Tumors growing in the peritoneum were excised, and one part of the tumor tissue was immediately frozen.

Statistical analysis

Statistical evaluation of the differential analysis was performed by one-way analysis of variance and Student's *t*-test. The threshold for statistical significance was set at $P < 0.05$.

CONFLICT OF INTEREST

LM received research grants from Karo Bio AB to support and develop her studies; and SN is a Karo Bio employee. The remaining authors declare no conflict of interests.

ACKNOWLEDGEMENTS

We acknowledge Dr Elisabet Kallin for 3PO synthesis and Dr Michele Cilli for *in vivo* experiments. This work was supported by Mesothelioma Applied Research Foundation (MARF grant 2009), Fondazione Buzzi Unicem, Italian Ministry of Economy and Finance to the CNR for the Project "FaReBio di Qualita' and Karo Bio AB (Huddinge, Sweden). KB9520 and 3PO were provided by Karo Bio AB (Huddinge, Sweden).

REFERENCES

1 Enmark E, Pelto-Huikko M, Grandien K, Lagercrantz S, Lagercrantz J, Fried G *et al.* Human estrogen receptor beta-gene structure, chromosomal localization, and expression pattern. *J Clin Endocrinol Metab* 1997; **82**: 4258–4265.
2 Gustafsson JÅ. Estrogen receptor beta-getting in on the action? *Nat Med* 1997; **3**: 493–494.
3 Mancuso M, Leonardi S, Giardullo P, Pasquali E, Borra F, Stefano ID *et al.* The estrogen receptor beta agonist diarylpropionitrile (DPN) inhibits medulloblastoma development via anti-proliferative and pro-apototic pathways. *Cancer Lett* 2011; **308**: 197–202.
4 Nilsson S, Gustafsson JÅ. Estrogen receptors: therapies targeted to receptor subtypes. *Clin Pharmacol Ther* 2011; **89**: 44–55, Review.
5 Sareddy GR, Nair BC, Gonugunta VK, Zhang QG, Brenner A, Brann DW *et al.* Therapeutic significance of estrogen receptor β agonists in gliomas. *Mol Cancer Ther* 2012; **5**: 1174–1182.
6 Carroll VM, Jeyakumar M, Carlson KE, Katzenellenbogen JA. Diarylpropionitrile (DPN) enantiomers: synthesis and evaluation of estrogen receptor β-selective ligands. *J Med Chem* 2012; **55**: 528–537.
7 Hughes ZA, Liu F, Platt BJ, Dwyer JM, Pulicicchio CM, Zhang G *et al.* WAY-200070, a selective agonist of estrogen receptor beta as a potential novel anxiolytic/antidepressant agent. *Neuropharmacology* 2008; **54**: 1136–1142.
8 Minutolo F, Macchia M, Katzenellenbogen BS, Katzenellenbogen JA. Estrogen receptor β ligands: recent advances and biomedical applications. *Med Res Rev* 2011; **31**: 364–442.
9 Muthusamy S, Andersson S, Kim HJ, Butler R, Waage L, Bergerheim U *et al.* Estrogen receptor β and 17β-hydroxysteroid dehydrogenase type 6, a growth

regulatory pathway that is lost in prostate cancer. *Proc Natl Acad Sci USA* 2011; **108**: 20090–20094.
10 Nilsson S, Koehler KF, Gustafsson JÅ. Development of subtype-selective oestrogen receptor-based therapeutics. *Nat Rev Drug Discov* 2011; **10**: 778–792, Review.
11 Parker Jr DL, Meng D, Ratcliffe RW, Wilkening RR, Sperbeck DM, Greenlee ML *et al.* Triazolo-tetrahydrofluorenones as selective estrogen receptor beta agonists. *Bioorg Med Chem Lett* 2006; **16**: 4652–4656.
12 Weiser MJ, Wu TJ, Handa RJ. Estrogen receptor-beta agonist diarylpropionitrile: biological activities of R- and S-enantiomers on behavior and hormonal response to stress. *Endocrinology* 2009; **150**: 1817–1825.
13 Wilkening RR, Ratcliffe RW, Tynebor EC, Wildonger KJ, Fried AK, Hammond ML *et al.* The discovery of tetrahydrofluorenones as a new class of estrogen receptor beta-subtype selective ligands. *Bioorg Med Chem Lett* 2006; **16**: 3489–3494.
14 Marzioni M, Torrice A, Saccomanno S, Rychlicki C, Agostinelli L, Pierantelli I *et al.* An oestrogen receptor β-selective agonist exerts anti-neoplastic effects in experimental intrahepatic cholangiocarcinoma. *Dig Liver Dis* 2012; **44**: 134–142.
15 Yakimchuk K, Iravani M, Hasni MS, Rhönnstad P, Nilsson S, Jondal M *et al.* Effect of ligand-activated estrogen receptor β on lymphoma growth in vitro and in vivo. *Leukemia* 2011; **25**: 1103–1110.
16 Pinton G, Brunelli E, Murer B, Puntoni R, Puntoni M, Fennell DA *et al.* Estrogen receptor-beta affects the prognosis of human malignant mesothelioma. *Cancer Res* 2009; **69**: 4598–4604.
17 Pinton G, Thomas W, Bellini P, Manente AG, Favoni RE, Harvey BJ *et al.* Estrogen receptor β exerts tumor repressive functions in human malignant pleural mesothelioma via EGFR inactivation and affects response to gefitinib. *PLoS One* 2010; **5**: e14110.
18 Campbell NP, Kindler HL. Update on malignant pleural mesothelioma. *Semin Respir Crit Care Med* 2011; **32**: 102–110, Review.
19 Kazan-Allen L. Asbestos and mesothelioma: worldwide trends. *Lung Cancer* 2005; **49**: S3–S8.
20 Yang H, Rivera Z, Jube S, Nasu M, Bertino P, Goparaju C *et al.* Programmed necrosis induced by asbestos in human mesothelial cells causes high-mobility group box 1 protein release and resultant inflammation. *Proc Natl Acad Sci USA* 2010; **107**: 12611–12616.
21 Kaufman AJ, Pass HI. Current concepts in malignant pleural mesothelioma. *Exp Rev Anticancer Ther* 2008; **8**: 293–303, Review.
22 Tsiouris A, Walesby RK. Malignant pleural mesothelioma: current concepts in treatment. *Nat Clin Pract Oncol* 2007; **4**: 344–352, Review.
23 Scherpereel A, Astoul P, Baas P, Berghmans T, Clayson H, de Vuyst P *et al.* Guidelines of the European Respiratory Society and the European Society of Thoracic Surgeons for the management of malignant pleural mesothelioma. European Respiratory Society/European Society of Thoracic Surgeons Task Force. *Eur Respir J* 2010; **35**: 479–495.
24 Blayney JK, Ceresoli GL, Castagneto B, O'Brien ME, Hasan B, Sylvester R *et al.* Response to chemotherapy is predictive in relation to longer overall survival in an individual patient combined-analysis with pleural mesothelioma. *Eur J Cancer* 2012; **48**: 2983–2992.
25 Ray M, Kindler HL. Malignant pleural mesothelioma: an update on biomarkers and treatment. *Chest* 2009; **136**: 888–896, Review.
26 Robinson BW, Lake RA. Advances in malignant mesothelioma. *N Engl J Med* 2005; **353**: 1591–1603.
27 Vander Heiden MG, Cantley LC, Thompson CB. Understanding the Warburg effect: the metabolic requirements of cell proliferation. *Science* 2009; **324**: 1029–1033, Review.
28 Koppenol WH, Bounds PL, Dang CV. Otto Warburg's contributions to current concepts of cancer metabolism. *Nat Rev Cancer* 2011; **11**: 325–337Review.
29 Grüning NM, Lehrach H, Ralser M. Regulatory crosstalk of the metabolic network. *Trends Biochem Sci* 2010; **35**: 220–227, Review.
30 Kroemer G, Pouyssegur J. Tumor cell metabolism: cancer's Achilles' heel. *Cancer Cell* 2008; **13**: 472–482.
31 Jose C, Bellance N, Rossignol R. Choosing between glycolysis and oxidative phosphorylation: a tumor's dilemma? *Biochim Biophys Acta* 2011; **1807**: 552–561.
32 Porporato PE, Dhup S, Dadhich RK, Copetti T, Sonveaux P. Anticancer targets in the glycolytic metabolism of tumors: a comprehensive review. *Front Pharmacol* 2011; **2**: 49.
33 Dröse S, Bleier L, Brandt U. A common mechanism links differently acting complex II inhibitors to cardioprotection: modulation of mitochondrial reactive oxygen species production. *Mol Pharmacol* 2011; **79**: 814–822.
34 Hargreaves IP, Duncan AJ, Wu L, Agrawal A, Land JM, Heales SJ. Inhibition of mitochondrial complex IV leads to secondary loss complex II-III activity: implications for the pathogenesis and treatment of mitochondrial encephalomyopathies. *Mitochondrion* 2007; **7**: 284–287.
35 Benard G, Trian T, Bellance N, Berger P, Lavie J *et al.* Adaptative capacity of mitochondrial biogenesis and of mitochondrial dynamics in response to pathogenic respiratory chain dysfunction. *Antioxid Redox Signal* 2012, epub ahead of print Apr **19**: 350–365.
36 Hansson A, Hance N, Dufour E, Rantanen A, Hultenby K, Clayton DA *et al.* A switch in metabolism precedes increased mitochondrial biogenesis in respiratory chain-deficient mouse hearts. *Proc Natl Acad Sci USA* 2004; **101**: 3136–3141.
37 Michel S, Wanet A, De Pauw A, Rommelaere G, Arnould T, Renard P. Crosstalk between mitochondrial (dys)function and mitochondrial abundance. *J Cell Physiol* 2011; **227**: 2297–2310.
38 Clem B, Telang S, Clem A, Yalcin A, Meier J, Simmons A *et al.* Small-molecule inhibition of 6-phosphofructo-2-kinase activity suppresses glycolytic flux and tumor growth. *Mol Cancer Ther* 2008; **7**: 110–120.
39 Oyedotun KS, Lemire BD. The quaternary structure of the *Saccharomyces cerevisiae* succinate dehydrogenase. Homology modeling, cofactor docking, and molecular dynamics simulation studies. *J Biol Chem* 2004; **279**: 9424–9431.
40 Horváth R, Abicht A, Holinski-Feder E, Laner A, Gempel K, Prokisch H *et al.* Leigh syndrome caused by mutations in the flavoprotein (Fp) subunit of succinate dehydrogenase (SDHA). *J Neurol Neurosurg Psychiatry* 2006; **77**: 74–76.
41 Astuti D, Latif F, Dallol A, Dahia PL, Douglas F, George E *et al.* Gene mutations in the succinate dehydrogenase subunit SDHB cause susceptibility to familial pheochromocytoma and to familial paraganglioma. *Am J Hum Genet* 2001; **69**: 49–54.
42 Bott M, Brevet M, Taylor BS, Shimizu S, Ito T, Wang L *et al.* The nuclear deubiquitinase BAP1 is commonly inactivated by somatic mutations and 3p21.1 losses in malignant pleural mesothelioma. *Nat Genet* 2011; **43**: 668–672.
43 Fornuskova D, Stiburek L, Wenchich L, Vinsova K, Hansikova H, Zeman J. Novel insights into the assembly and function of human nuclear-encoded cytochrome c oxidase subunits 4, 5a, 6a, 7a and 7b. *Biochem. J* 2010; **428**: 363–374.
44 Hayashi R. Expression and regulation of an estrogen-responsive gene, cytochrome c oxidase subunit 7a related polypeptide (COX7RP) in endometrial cancer. *Saitama Ika Daigaku Zasshi* 2004; **31**: 199–206.
45 Dager SR, Friedman SD, Parow A, Demopulos C, Stoll AL, Lyoo IK *et al.* Brain metabolic alterations in medication-free patients with bipolar disorder. *Arch Gen Psychiatry* 2004; **61**: 450–458.
46 Hu Y, Lu W, Chen G, Wang P, Chen Z, Zhou Y *et al.* K-ras(G12V) transformation leads to mitochondrial dysfunction and a metabolic switch from oxidative phosphorylation to glycolysis. *Cell Res* 2011; **22**: 399–412.
47 Smythe WR, Kaiser LR, Hwang HC, Amin KM, Pilewski JM, Eck SJ *et al.* Successful adenovirus mediated gene transfer in an *in vivo* model of human malignant mesothelioma. *Ann Thorac Surg* 1994; **57**: 1395–1401.
48 Williams C, Edvardsson K, Lewandowski SA, Ström A, Gustafsson JA. A genome-wide study of the repressive effects of estrogen receptor beta on estrogen receptor alpha signaling in breast cancer cells. *Oncogene* 2008; **27**: 1019–1032.
49 Chomczynski P, Sacchi N. Single-step method of RNA isolation by acid guanidinium thiocyanate-phenol-chloroform extraction. *Anal Biochem* 1987; **162**: 156–159.
50 Chen J, Kadlubar FF, Chen JZ. DNA supercoiling suppresses real-time PCR: a new approach to the quantification of mitochondrial DNA damage and repair. *Nucleic Acids Res* 2007; **35**: 1377–1388.
51 Valenti D, Manente GA, Moro L, Marra E, Vacca RA. Altered cAMP-dependent phosphorylation of mitochondrial complex I determines deficit of the complex activity and overproduction of reactive oxygen species by mitochondria in human skin fibroblasts with chromosome 21 trisomy. *Biochem J* 2011; **435**: 679–688.
52 Valenti D, Tullo A, Caratozzolo MF, Merafina RS, Scartezzini P, Marra E *et al.* Impairment of F1FO-ATPase, adenine nucleotide translocator, and adenylate kinase causes mitochondrial energy deficit in human skin fibroblasts with chromosome 21 trisomy. *Biochem J* 2010; **431**: 299–310.
53 Chelli B, Lena A, Vanacore R, Da Pozzo E, Costa B, Rossi L *et al.* Peripheral benzodiazepine receptor ligands: mitochondrial transmembrane potential depolarization and apoptosis induction in rat C6 glioma cells. *Biochem Pharmacol* 2004; **1**: 125–134.
54 Maftah A, Petit JM, Ratinaud MH, Julien R. 10-N nonyl-acridine orange: a fluorescent probe which stains mitochondria independently of their energetic state. *Biochem Biophys Res Commun* 1989; **164**: 185–190.

Supplementary Information accompanies this paper on the Oncogenesis website (http://www.nature.com/oncsis).